IEEE Access
Multidisciplinary | Rapid Review | Open Access Journal

Received September 18, 2020, accepted September 24, 2020, date of publication October 1, 2020, date of current version October 15, 2020.

Digital Object Identifier 10.1109/ACCESS.2020.3028134

Rectangular Cavity Sensor for Distinguishing Between Normal and High-Drivability-Index Gasolines

CHONG HYUN LEE, (Member, IEEE), YOONSANG JEONG, AND HINA ASHRAF
Department of Ocean System Engineering, Jeju National University, Jeju 690-756, South Korea

Corresponding author: Chong Hyun Lee (chonglee@jejunu.ac.kr)

This work was supported by the National Research Foundation of Korea (NRF) through the Basic Science Research Program funded by the Ministry of Science, ICT and Future Planning under Grant NRF-2017R1A2B4003705.

ABSTRACT The Drivability Index (DI) of gasoline is a measure of fuel performance of engine operations. Therefore, distinguishing a gasoline of specific DI in advance is useful for improving engine efficiency and maintenance. We consider the problem of distinguishing between normal gasoline and HiDI (High DI) gasolines and propose an electromagnetic wave-based rectangular cavity sensor. For commercialization, it is designed to have a simple structure and basic resonance mode TM_{110} in the common frequency range of 5 GHz to 6 GHz. The proposed sensor has a simple structure of monopole radiating electromagnetic waves and a metal rectangular cavity containing gasoline samples. By considering one commercial normal gasoline sample of permittivity 2.157 and five HiDI gasoline samples of permittivity in the range of 2.018 to 2.218, we obtain 11.5 MHz resonance separation at room temperature to the closest HiDI sample from the simulation and 8 MHz resonance separation from the fabricated sensor experiment. To verify the feasibility of the fabricated sensor under temperature variation from 0°C to 20°C, we derived a simple linear distinction function of resonance frequency and S11 parameter and obtained a minimum 4.4MHz resonance separation. These results showed that the distinction performance for normal gasoline is robust to temperature variations. Furthermore, we showed that the distinction property is robust to design parameter errors, installation position variations and sensing time variations. These results show that the proposed sensor can be utilized effectively for distinguishing normal gasoline.

INDEX TERMS Cavity resonator sensor, DI (drivability index), gasoline, permittivity, resonance, S11 parameter frequency.

I. INTRODUCTION

Gasoline, also referred to as gasolene, is a homogeneous mixture of volatile chemical constituents used as fuel for internal combustion engines [1]. It is well-known to automobile engineers that the volatility of gasoline plays a critical role in affecting vehicle drivability and operation [2]. The DI index is defined as the temperature at which specified fractions of the sample are distilled, and it is closely related to volatility. An appropriate drivability index leads to smooth acceleration, ease in engine cold-start/warm-up operations and no or far less surge while driving. A sufficient amount of gasoline is required to initiate combustion; otherwise, incomplete combustion may lead to unnecessary emission and exhaustion due to the additional hydrocarbons from the unburned portion of gasoline [3]. The design of the HiDI sensor can be of great assistance in properly adjusting the air-to-fuel ratio before combustion. To make such a sensor robust, it must quickly perform measurements and be small in size. These features would allow it to be easily mounted inside the fuel inlet or the fuel tank.

Most DI sensors measure fuel volatility by measuring the temperature or the rate of fuel level as a function of the fuel temperature after combustion. Recently, DI estimation was performed in the study presented by Lambert *et al.* [4] These researchers placed gasoline samples between parallel aligned capacitor plates. This sample was then heated, and the change in capacitance of the sensing element was measured in reference to time and temperature [4]. Another study approximated the volatility of low and high DI gasoline during cold starts, utilizing wide range platinum resistance temperature detectors (RTDs) to relate the temperatures of engine out exhaust gas to definite engine out exhaust air/gasoline ratios [5]. Moreover, an algorithm for fuel delivery corrections by monitoring fuel combustion in a cylinder is reported [6]. This technique consumes fuel and has a long latency

The associate editor coordinating the review of this manuscript and approving it for publication was Ming Luo.

time for fuel combustion and heating. Therefore, sensors based on microwaves become better candidates, since they are nondestructive, enable compact size configurations for fitting inside fuel tanks and take significantly less time for detection.

Recently, myriad studies have offered microwave-based techniques for the identification and observation of numerous liquid samples [7]–[12]. These techniques offer a cost-effective and simple solution to the sensing problem where sensing takes place due to the interaction between the sample and resonating modes of electromagnetic waves. This interaction results in changing the dielectric of the observed sample which, in turn, changes the signal frequency, phase and amplitude or causes reflection. Hence, by determining changes in resonance frequency, reflection and transmission coefficients according to the contents inside the cavity, various materials can be characterized.

Following this principle, cavity designs have been widely used for measuring the permittivity of the object because of their high quality (Q) factor [13]. Oon *et al.* [14] analyzed a two-phase gas–liquid flow regime in a pipeline using a difference in permittivity according to the change in the ratio of water and air components. Therefore, the change in permittivity according to the ratio of components is very large, making it a less sensitive sensor.

Other than the high Q factor, resonant cavities offer such advantages as easy fabrication, minimal sample requirement, greater accuracy due to their resonant characteristics [15], [16] and better sensitivity [17] when resonant frequency points are considered explicitly. A sensor based on waveguide cavity shape was proposed for chemical liquid sensing by Memon and Lim [18]. Similarly, Karuppuswami *et al.* [19] proposed a rectangular cavity sensor fabricated by a 3D printer for liquid detection. Following the cavity design, a cylindrical cavity sensor for gasoline DI distinction was proposed by Lee *et al.* [20].

In this article, a microwave-based sensor for the distinction of normal gasoline from HiDI gasolines is proposed. The as-developed sensor design is based on a rectangular metal cavity enclosure, which results in a small size and easy fabrication. The designed sensor was experimentally verified and demonstrated using an ANSYS high-frequency structure simulator (HFSS) and a vector network analyzer (VNA), which shows the consistency of the simulations with experiments. Additionally, the robustness of the sensor to temperature variations was also verified by conducting different experiments. The sensor shows an obvious change in resonance frequency with the change in DI, which can be effectively used for the distinction of normal gasoline and HiDI gasoline.

There are three main contributions of the proposed sensor: the first is its ability to distinguish various gasolines despite the very small difference in relative permittivity (2.018 to 2.218) with minimum 4.4 MHz resonance separation; the second is its robustness towards temperature variations for the distinction of normal and HiDI gasolines without any significant compromise on sensitivity and accuracy; the third is its reliability and stability to design errors and installation position errors.

Our paper is organized as follows. Section 2 describes the rectangular cavity theory and sensor modeling along with an error analysis of the sensor via simulations and experiments. In Section 3, the sensor fabrication and experimental results, as well as a linear function for normal gasoline distinction, are described. In Section 4, the final conclusion of the paper is presented.

II. SENSOR MODELING AND DESIGN

A. THEORY AND PRINCIPLE OF OPERATION

The operating principle of microwave-based sensors depends on the interaction of electromagnetic (EM) waves with the material under analysis. Due to this interaction, the test material alters the signal velocity, causing reflection or attenuation. One of the main advantages of such sensors is their ability to safely measure in an enclosure without any external interaction using only EM penetrating waves. When the cavity is excited with an appropriate frequency, it starts to resonate, causing different resonance modes to occur. These resonance mode frequencies depend on the structural parameters of the resonator cavity and the dielectric properties of the sample inside. In a rectangular waveguide, TEM mode cannot occur, and the only propagating modes are TE and TM, in which the resonant frequency can be calculated using Equation (1) [21].

$$f_{mnl} = \frac{c}{2\sqrt{\mu_r \varepsilon_r}} \sqrt{\left(\frac{m}{a}\right)^2 + \left(\frac{n}{b}\right)^2 + \left(\frac{l}{d}\right)^2} \tag{1}$$

where m, n, l are the mode numbers; c is the speed of light; μ_r denotes the relative permeability (since the gasoline samples are nonmagnetic, the value is taken to be 1); ε_r is the relative permittivity of the sample and a, b, d are the width, height and depth of the cavity, respectively. For TM modes, the values $m = n = 0$ are not a possible combination; therefore, the lowest frequency mode with stable resonant frequency for the rectangular cavity is TM_{110}. It is desirable to have a maximum intensity of the magnetic field and minimum intensity of the electric field where the sample is present. A higher magnetic field results in effective excitation and an increased signal-to-noise ratio (SNR), while a higher electric field deposits higher power, which leads to sample heating. The condition is further worsened if the sample is conductive [21].

The Q value of the cavity sensor can be largely defined as the loss Q_{mnl} due to the cavity wall and Q_{3dB} representing the sharpness of resonance. The loss Q_{mnl} due to the cavity wall of the rectangular cavity resonator operating in m, n, l mode is given in Equation (2).

$$Q_{mnl} = \frac{Z_w abd k_{xy}^2 k_{mnl}}{4R_s \left[b\,(a+d)\,k_x^2 + a(b+d)k_y^2\right]} \left(k_x = m\frac{\pi}{a}, k_y = n\frac{\pi}{b}, k_z = l\frac{\pi}{d}, k_{xy} = \sqrt{k_x^2 + k_y^2}, k_{mnl} = \sqrt{k_x^2 + k_y^2 + k_z^2}\right) \tag{2}$$

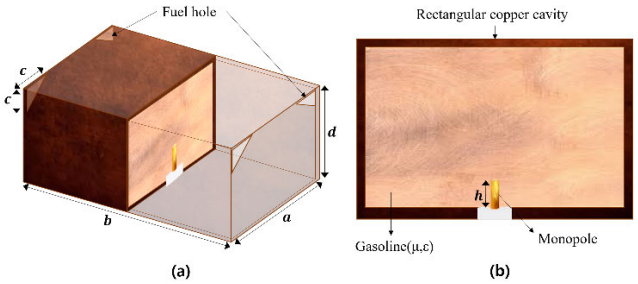

FIGURE 1. Geometry of the proposed sensor. (a) Isometric view, (b) Side view.

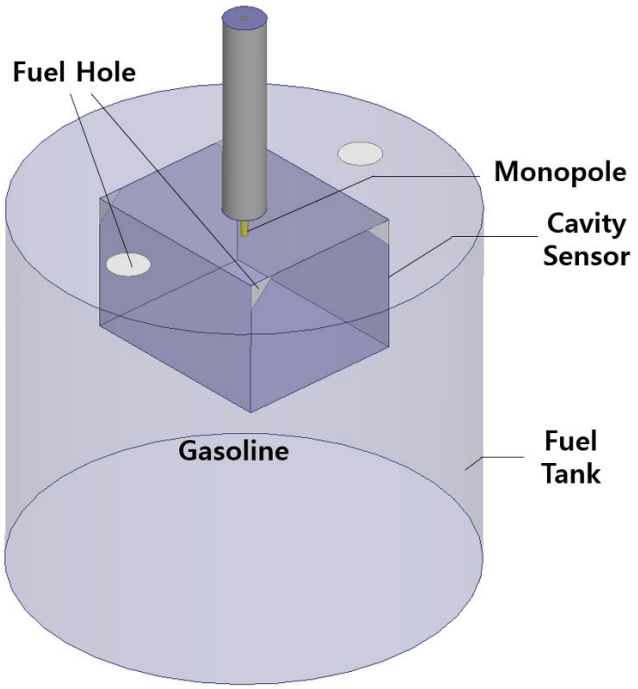

FIGURE 2. Simulation model.

where Z_w is the natural impedance of air and R_s is the surface resistance of the resonator wall. The higher the Q_{mnl}, the more energy is stored in the cavity compared to the power consumed by the cavity wall [22]. The sharpness of resonance Q_{3dB} is as shown in Equation (3) [23].

$$Q_{3dB} = \frac{f_r}{B} \cdots \tag{3}$$

In this equation, f_r is the resonance frequency, and B is the bandwidth, which is the difference between the two frequencies that are 3 dB higher than the reflection loss of the resonance frequency. The higher the Q_{3dB} value, the lower the return loss and narrow bandwidth; therefore, it is easy to distinguish gasoline samples. In this article, the process of optimizing the Q_{3dB} value of the sensor is performed through simulation during the design of the sensor.

The designed sensor model is shown in Fig. 1. The sensor is composed of two major components: a monopole and a rectangular cavity made up of copper enclosure filled with relative permittivity ε_r ($\varepsilon = \varepsilon_0\varepsilon_r$, where ε_0 and ε are the permittivities of free space and gasoline, respectively).

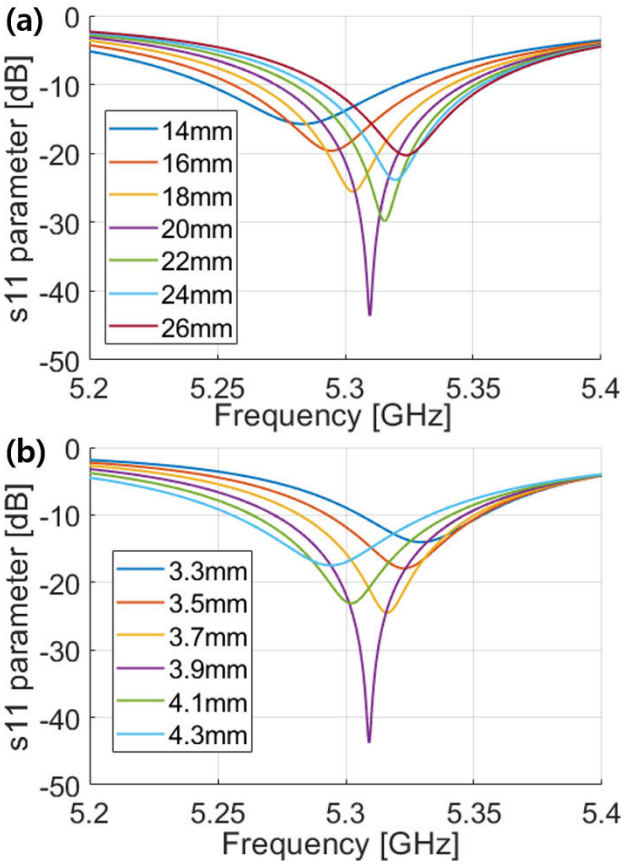

FIGURE 3. S11 parameters vs. (a) Sensor depth, d, (b) Monopole height, h.

TABLE 1. Optimized Sensor Parameters.

Parameter	Dimension (mm)	Parameter	Values
a	30	*Mode*	TM
b	25	*Mode numbers (mnl)*	110
d	20	*Resonant Frequency band*	5-6 GHz
h	3.9	*Permittivity (ε_r)*	2-2.2
e	4		

The interior of the rectangular cavity is hollow with a small feeding source vertically placed at the center for the transmission of EM waves. As described in (1), the cavity sensor exhibits a specific resonance mode according to the design parameters and sample permittivity. A thin protective layer of insulating medium is coated over the monopole to avoid corrosion and direct contact with the samples inside, which may cause unwanted results.

B. SENSOR DESIGN AND SIMULATION RESULTS

By using HFSS, the proposed sensor is designed to detect normal gasoline among various gasolines, including HiDI gasolines. The sensor is designed for commercialization and has a resonance band below 6 GHz, which is common operating frequency of commercial RF device. Moreover, the sensor is designed considering the characteristics of a rectangular resonator that increases the rate of change of the resonance frequency per relative permittivity and decreases the size of

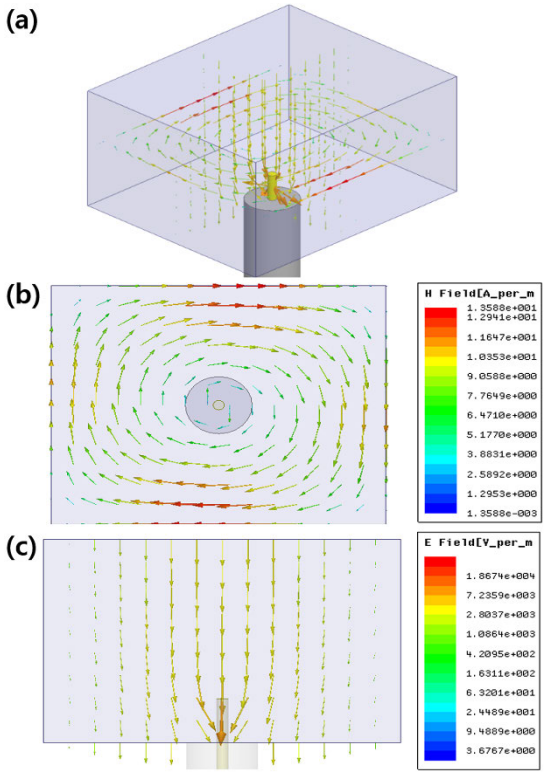

FIGURE 4. EM fields in TM_{110} mode. (a) EM field, (b) Top view of the M field, (c) Top view of the E field.

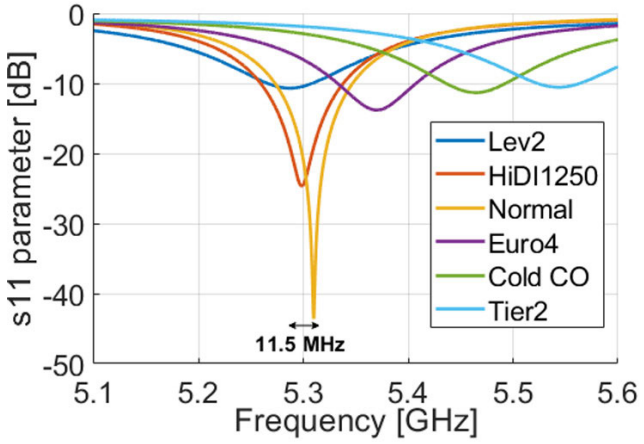

FIGURE 5. Frequency responses of normal and HiDI and gasolines with the designed sensor.

the sensor in the high frequency band, which is found to be 5∼6 GHz. The simulation model for the design of the sensor is shown in Fig. 2. The sensor is modeled as a structure contained in a fuel tank filled with gasoline. The dimensions of the sensor are optimized to have a basic TM_{110} resonance with a high Q_{3dB} value for the previously mentioned resonant frequency band. The design procedure of the proposed rectangular cavity sensor is as follows:

Enclosure width (a) and height (b): By setting the permittivity of normal gasoline to 2.157, the dimensions are designed to have a resonance frequency range from 5 GHz to 6 GHz. The dimensions are determined to have TM_{110} [13].

TABLE 2. Units for Electric Properties.

GASOLINE	DI	PERMITTIVITY	LOSS TANGENT [E"/E]
TIER2	1144	2.018	0.038
COLD CO	1132 [27]	2.072	0.036
EURO4	N/A	2.134	0.031
NORMAL	443 [4,27]	2.157	0.02
HIIDI1250	1255	2.173	0.023
LEV2	1168 [27]	2.218	0.042

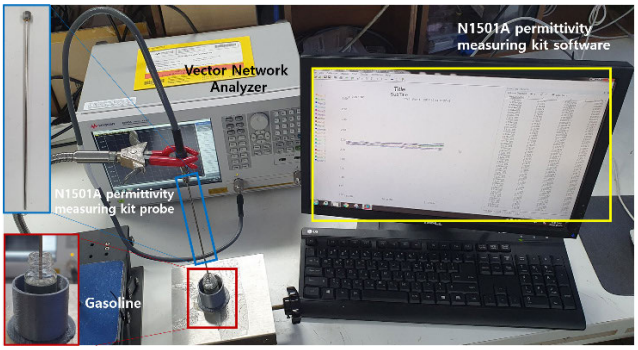

FIGURE 6. Setup for measuring permittivity at room temperature.

Enclosure depth (d): The frequency responses according to various depths are evaluated to examine the Q_{3dB} at TM_{110}. The optimum depth (d) can be obtained as shown in Fig. 3(a).

Monopole height (h): Similar to step 2, the height of the monopole is optimized to have a high Q_{3dB} at TM_{110}. The simulation results are shown in Fig. 3(b).

The design parameters of the proposed cavity sensor are summarized in Table 1. The optimized width, a, height, b, and depth, d, are set to be 30 mm, 25 mm and 20 mm, respectively. The monopole height, h, is 3.9 mm, and e is the edge length of the triangular hole.

The designed sensor is verified by using HFSS software, as shown in Figs. 4 and 5. It can be observed from Fig. 4 that the EM field at resonance frequency matches well with the designed TM_{110}. Note that the magnetic field of the TM mode is perpendicular to the sensor depth direction, and the order of the electric field is one to the width and height directions.

The frequency responses of the proposed sensor for HiDI and normal gasoline are plotted in Fig. 5. The permittivities and the corresponding loss tangents are summarized in Table 2. These values are measured at room temperature (19°C∼21°C) by using an N1501A permittivity measuring kit by KEYSIGNT Technology, and the average of 5 measurements taken from the measurement system is measured. The corresponding experimental environment for measuring the permittivity is shown in Fig. 6.

The minimum permittivity difference between normal and HiDI gasolines is as small as 0.016. Nevertheless, the resonance separation of the proposed sensor becomes at least 11.5 MHz, which is much higher than the 0.1 MHz frequency resolution of VNA. This large frequency margin, along with the high Q_{3dB} factor at normal gasoline resonance frequency show the validity of the proposed sensor plausible.

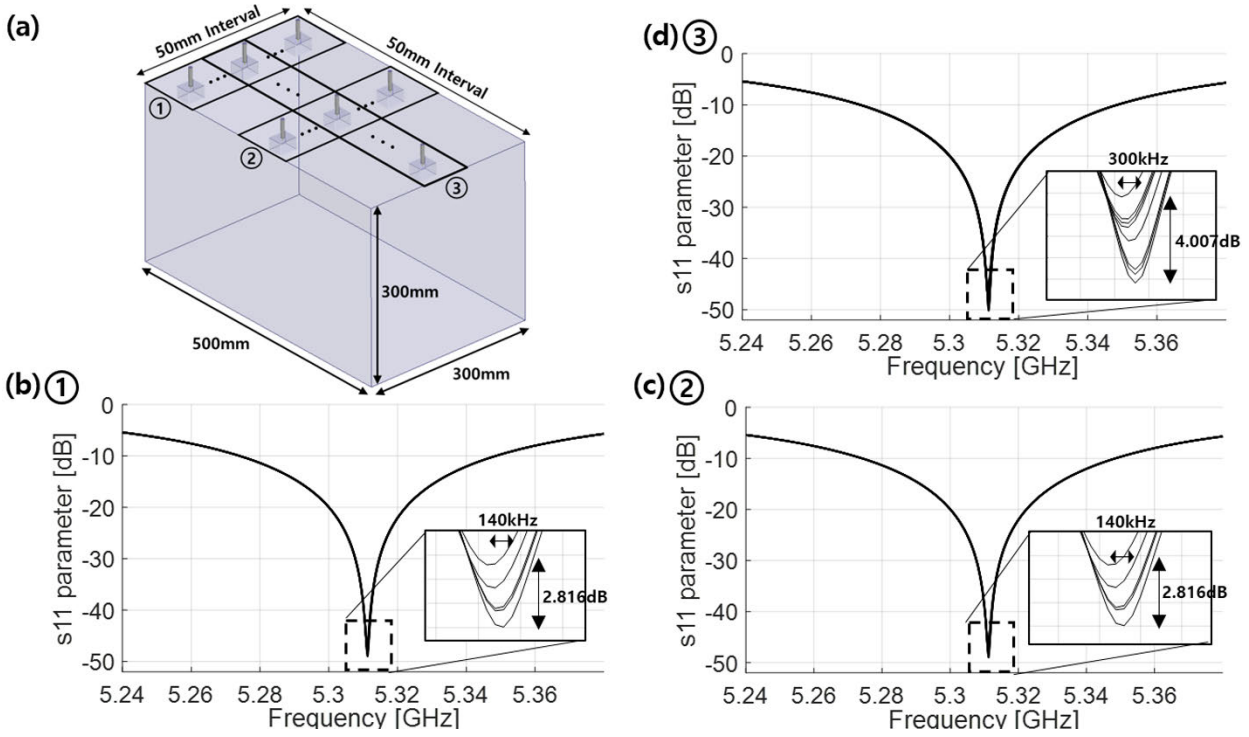

FIGURE 7. (a) Simulation setup, (b) Frequency responses at position ①, (c) Frequency responses at position ②, (d) Frequency responses at position ③.

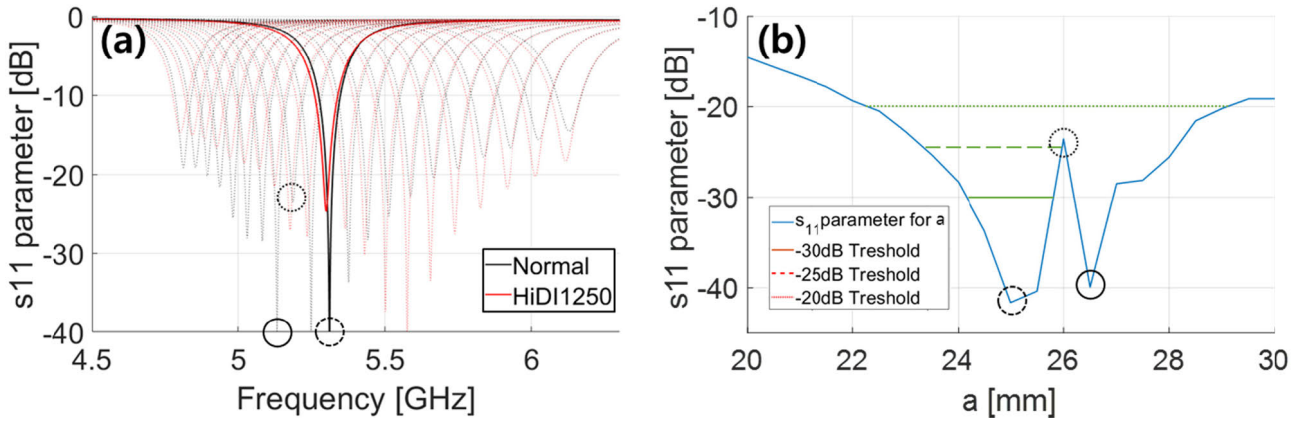

FIGURE 8. (a) Frequency responses according to size variations of a, (b) Minimum S11 vs. size variations of a.

C. SENSITIVITY ANALYSIS OF THE SENSOR

To verify the reliability of the designed sensor, we conducted a few simulations by changing the design parameters.

1) EFFECT OF SENSOR POSITION ON SENSING PROPERTY

To show that the resonant characteristics of the proposed sensor are robust to sensor positions, we consider a fuel tank of 45 L, which is full of normal gasoline. Next, we measure variations in resonance frequencies and S11 parameters by moving the sensor position by 50 mm. The obtained results are shown in Fig. 7, in which the resonance frequency shift and S11 difference are less than 300 kHz and 4.01 dB, respectively. These numbers reflect less than 0.0056% changes in resonance frequency and 8% changes in S11 parameters, which are negligible changes for normal gasoline distinction.

2) EFFECT OF SENSOR PARAMETERS ON SENSING PROPERTY

To determine the reliability of the proposed sensor, we have investigated sensing performance by considering errors in parameters given in Table 1. In this study, we only consider one parameter at a time while the other three parameters are fixed as optimum values. To evaluate the sensing property, we only consider the closest sample HiDI1250, instead of all samples, because the rest of the HiDI samples are far more separated than the HiDI1250. To set the threshold of two sample separations, we choose a 10 MHz frequency separation and consider three S11 parameter values of −20 dB, −25 dB and −30 dB.

By changing **a** size from 20 to 30 mm in 0.05-mm increments, we obtain resonance responses and evaluate

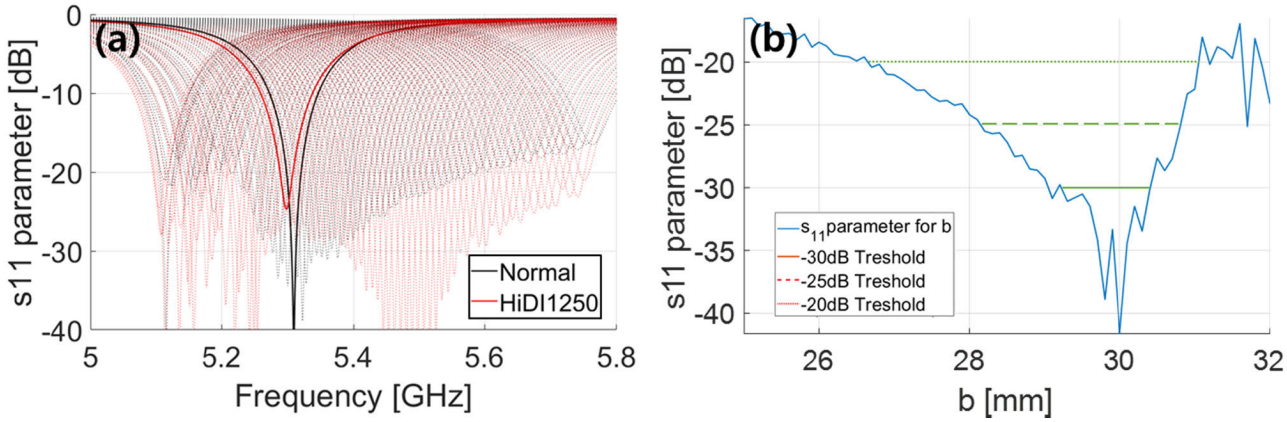

FIGURE 9. (a) Frequency responses according to size variations of b, (b) Minimum S11 vs. size variations of b.

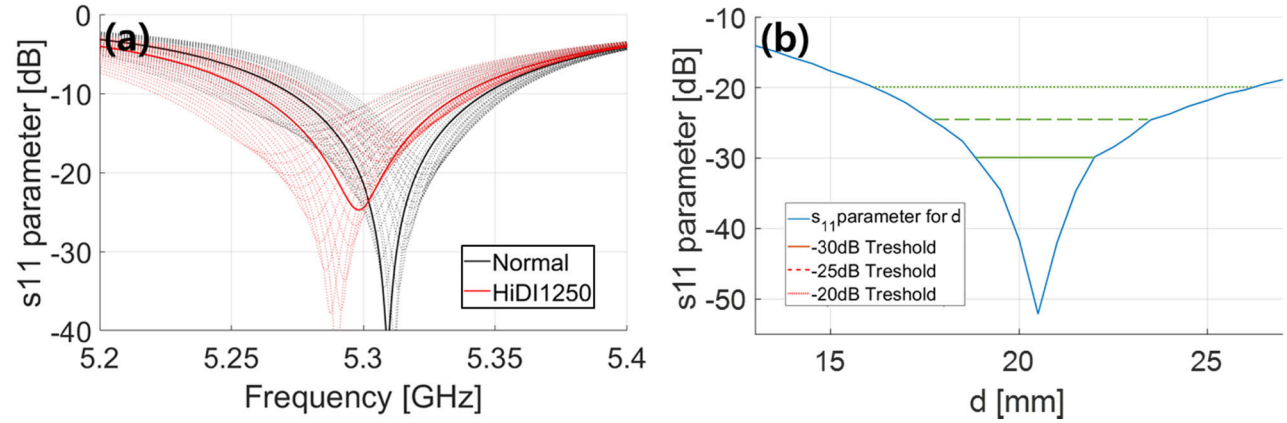

FIGURE 10. (a) Frequency responses according to size variations of d, (b) Minimum S11 vs. size variations of d.

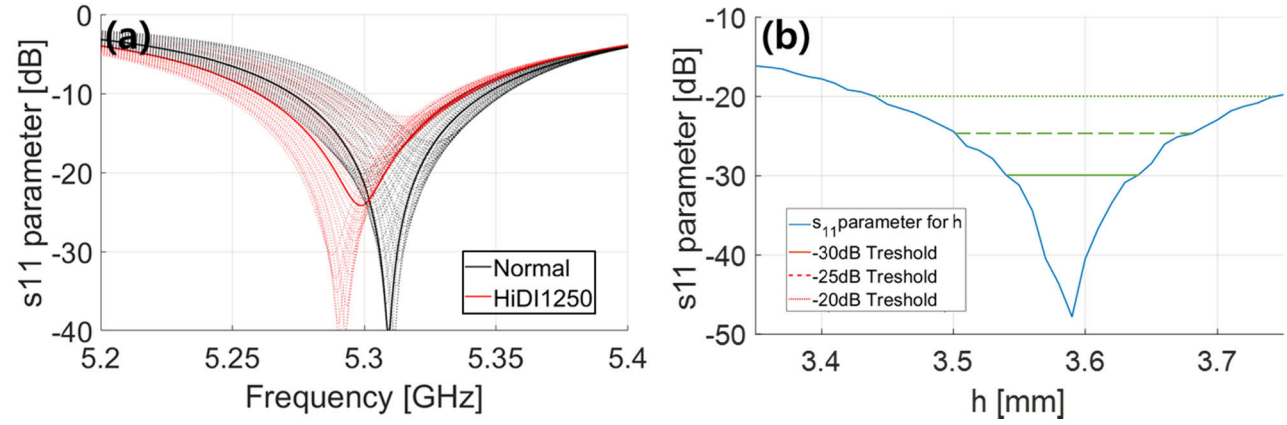

FIGURE 11. (a) Frequency responses according to size variations of h, (b) Minimum S11 vs. size variations of h.

resonance separation and minimum S11 parameters according to **a** size, which are shown in Fig. 8. Next, we obtain resonance responses and evaluate resonance separation and minimum S11 parameters according to **b** size, which are shown in Fig. 9 by changing **b** size from 25 to 32 mm in 0.1-mm increments. Similarly, we obtain resonance separation and minimum S11 parameters according to **d** sizes of 0.5 mm increments and to **h** sizes of 0.02 mm increments and present them in Figs. 10 and 11, respectively.

The tolerances of the **a, b, d** and **h** size errors according to the three S11 parameter thresholds are summarized in Table 3.

The evaluated minimum design margin at −30 dB is 3.7% in **b** size, and the maximum is 14.5% in **d** size. The minimum

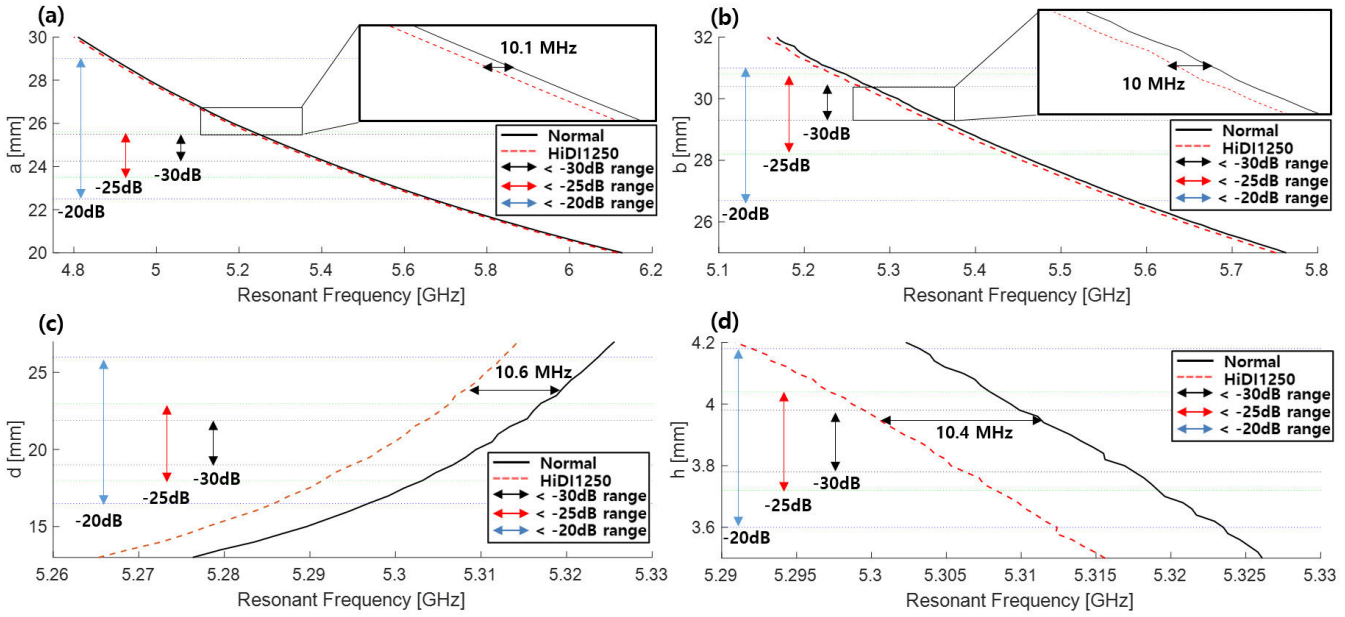

FIGURE 12. Resonance frequencies of normal and the closest HiDI vs. (a) size variations of a, (b) size variations of b, (c) size variations of d, (d) size variations of h.

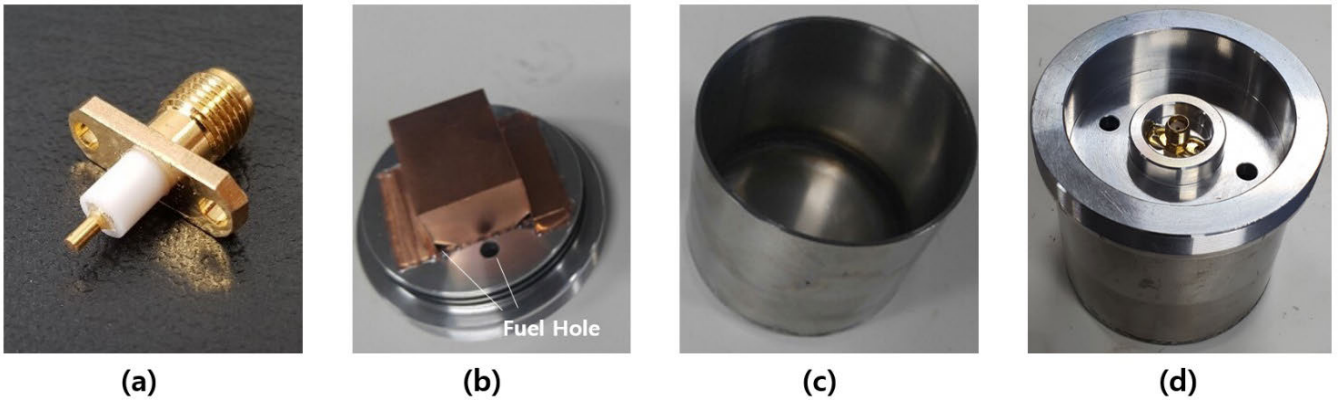

FIGURE 13. Manufactured sensor and tank. (a) Monopole, (b) Rectangular Cavity Sensor enclosure, (c) Fuel Tank, (d) Assembled form.

TABLE 3. Tolerance of Design Parameter Errors According to S11 Parameter Thresholds.

Design Parameter [mm]	S_{11} Threshold	-20 dB	-25 dB	-30 dB
a [25]	Δa [mm]	-2.5~4	-1.5~0.6	-0.75~0.5
	error [mm]/[%]	6.5/**26**	2.1/**8.4**	1.25/**5**
b [30]	Δb [mm]	-3.3~1	-1.8~0.8	-0.7~0.4
	error [mm]/[%]	4.3/**14.3**	2.6/**8.7**	1.1/**3.7**
d [20]	Δd [mm]	-3.5~6	-2~3	-1~1.9
	error [mm]/[%]	9.5/**47.5**	5/**25**	2.9/**14.5**
h [3.9]	Δh [mm]	-0.3~0.28	-0.18~0.14	-0.12~0.08
	error [mm]/[%]	0.58/**14.9**	0.32/**8.2**	0.2/**5.1**

and maximum design margins increase to 14.3% in **b** size and 47.5% in **d** size, respectively. Note that the minimum resonance separations under the **a, b, d** and **h** size errors are greater than the predefined 10 MHz threshold, as shown in Fig. 12. These results prove that the proposed sensor design is a reliable fabrication method.

3) EFFECT OF SENSOR PARAMETERS ON RESONANCE FREQUENCY

To check the stability (stable distinction) of the proposed sensor according to sensor size errors, we have investigated resonance frequencies of the closest sample HiDI1250 and normal gasoline. The frequency separations according to **a, b, d** and **h** size variations are shown in Fig. 12. From the figure, we can notice that the minimum 10 MHz separations are maintained at resonance frequencies for all considered design parameters. These results assure that the proposed sensor guarantees stable distinction of normal gasoline.

III. EXPERIMENTAL RESULTS AND DISCUSSION

A. SENSOR FABRICATION AND VERIFICATION

Based on the parameters in Section II, we fabricate the proposed sensor, as shown in Fig. 13. During the fabrication process, the length of the sensor monopole was adjusted

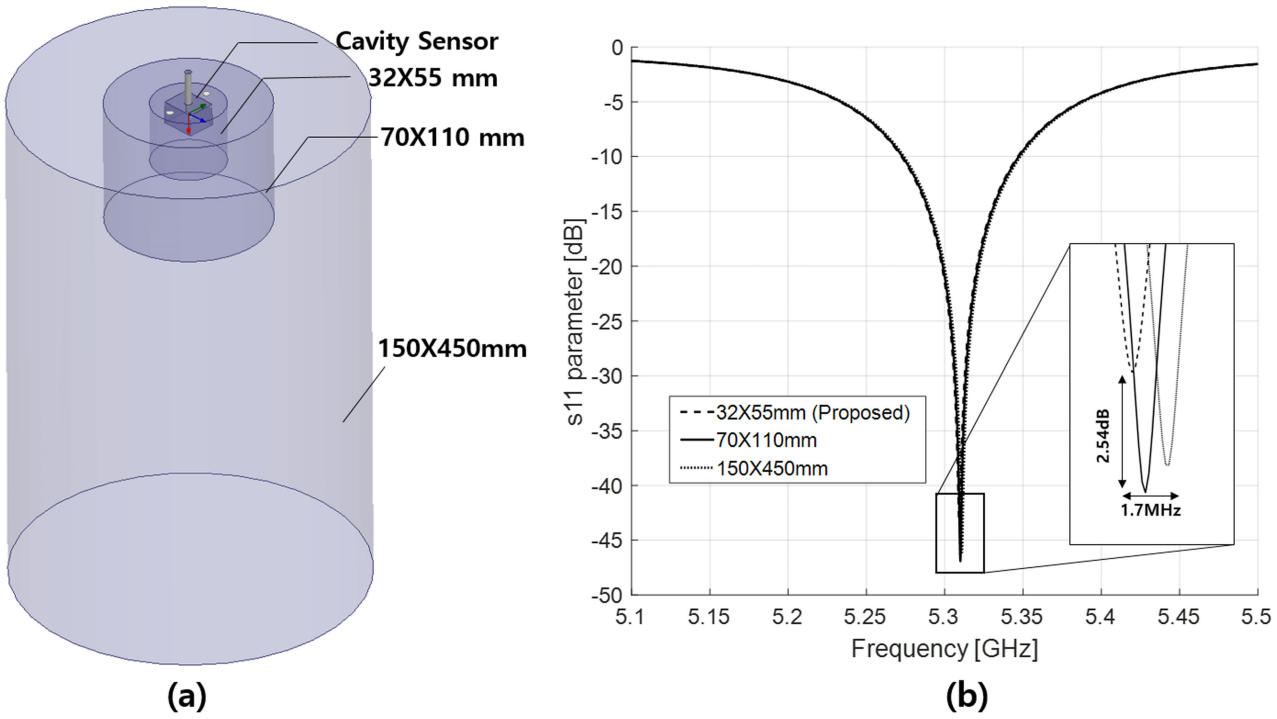

FIGURE 14. (a) Models of three fuel tanks, (b) Frequency responses of three fuel tanks.

from 3.9 to 3.7 mm to compensate the manufacturing error. The monopole of the sensor is fabricated using an SMA connector, and the enclosure is fabricated using a 0.3 mm copper plate. The sensor is attached to the top of the small aluminum fuel tank, in substitution for the car fuel tank. The tank is a cylindrical aluminum case with a size of 32×55 mm (radius×height) tightened to the sensor with a rubber ring. The gasoline is injected with a motor pump through the two circular fuel holes at the top of the tank until the sensor is sunk under gasoline. The gasoline reaches the sensor through triangular fuel holes with edge dimensions (e) of 4 mm.

The sensor is a shielded cavity sensor; therefore, theoretically, the fuel size does not affect the sensitivity of the sensor. To verify insensitivity, the simulation model and results with different fuel tank sizes are shown in Fig. 14. In simulations, three size of the fuel tanks are considered such as 32×55 mm (the proposed size), 64×110 mm (twice of the proposed size) and 150×450 mm (equivalent to 31.8 L fuel tank, $150^2 \times \pi \times 450 = 31{,}808{,}625$ mm^3). The resonance frequency of the proposed sensor is 5.3074 GHz, and the reflection coefficient is -43.58 dB when the proposed 32×55 mm fuel tank is considered. Note that the difference in resonance frequency and reflection coefficients for three fuel tanks is less than 1.7 MHz and 2.54 dB, respectively. These results show that the sensor performance is insensitive to the outside fuel tank size.

The measured average frequency response of the fabricated sensor with S11 parameters according to various gasoline samples at room temperature (19°∼21°) is shown in Fig. 15.

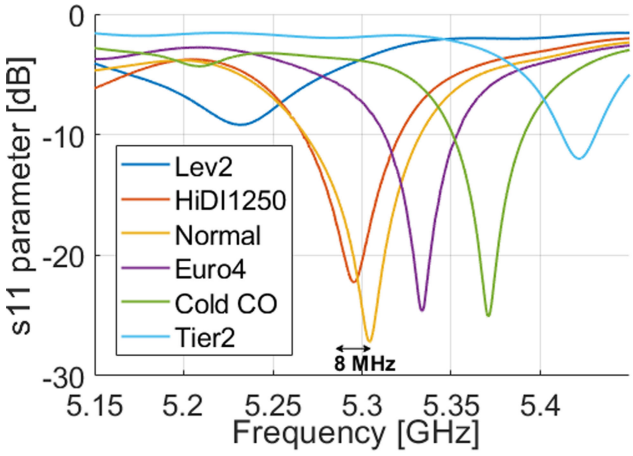

FIGURE 15. Frequency responses of normal and HiDI gasolines with the fabricated sensor.

The S11 parameter for normal gasoline at resonance frequency increases from -36.7 dB to -26.9 dB, which it is still lower than other resonance frequencies of HiDI gasolines. The minimum frequency separation among resonance frequencies of HiDI gasoline is measured as 8 MHz, which is sufficient for the distinction of HiDI gasolines. Additionally, note that the 8 MHz frequency margin can guarantee distinction of normal gasoline even when 0.1 MHz of max frequency deviation of five measurements is considered.

To verify the resonance frequency relation with permittivity, as given in Equation (1), HFSS simulation and experiments were performed at room temperature. The resonance

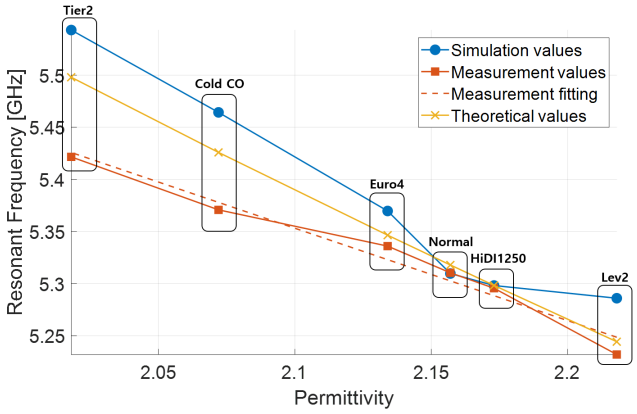

FIGURE 16. Simulated, experimental and theoretical results of different gasoline samples at room temperature.

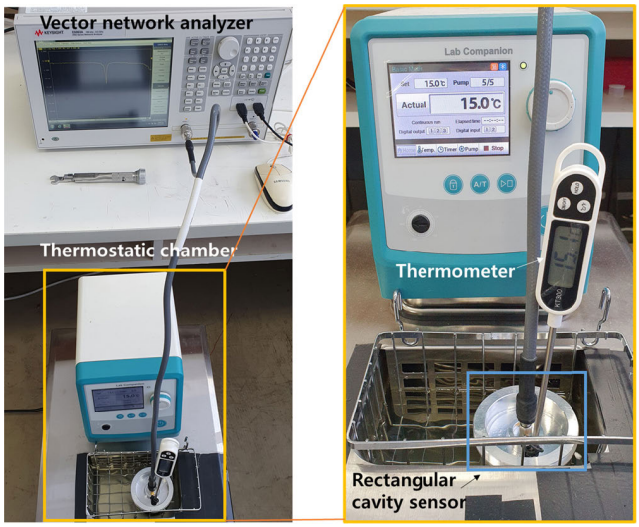

FIGURE 17. Actual experimental setup for various temperature settings.

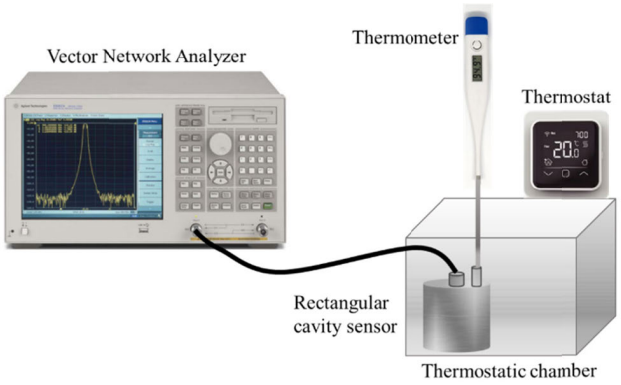

FIGURE 18. Schematics of the experimental setup for various temperature settings.

changes are displayed in Fig. 16, which shows that the measurements decrease as permittivity increases. The 39 MHz of average resonance frequency deviation from the simulations can be explained by experimental and fabrication errors. Nevertheless, we can observe that the proposed sensor exhibits remarkable resonance frequency to unity permittivity ratio as 931 MHz/ε by computing the slope of the dotted measurement fitting line.

B. EXPERIMENT AT VARIOUS TEMPERATURES

When there is a variation in temperature, it also affects the permittivity of the solution, which subsequently changes the resonant frequency of a permittivity-based sensor. For hydrocarbon oils, including gasoline, the change in permittivity with temperature can be calculated following Equation (4), where t is the temperature of the gasoline sample, ε_{20} is the relative permittivity at 20°, and α is the relative permittivity change coefficient that typically ranges from 0.0013 to 0.05% per degree Celsius [24]. For our case, working within the operating frequency of 5 GHz to 6 GHz, increasing the temperature decreases the relative permittivity of normal gasoline ranging from 2.157 to 2.155.

$$\varepsilon\,(t) = \varepsilon_{20}(1 - \alpha(t - 20)) \tag{4}$$

The experimental setup for evaluating the distinction capability of the proposed sensor under different temperatures is shown in Fig. 17. The corresponding experimental schematics to measure the resonant frequency at different temperatures are shown in Fig. 18 for the purpose of clarity. In this setup, the sensor is placed in a thermostatic chamber to provide varying temperature conditions using a thermostat. The sensor is connected to a VNA (100 kHz-8.5 GHz, E5063A, KEYSIGHT) via a 50Ω coaxial cable and to a thermostatic bath. The temperature variations were observed from 0° to 20° with a 5° step size increment. To validate the sensing performance of the proposed sensor over repetitive experiments, we measured resonance frequencies and S11 parameters of six samples five times at 5-minute intervals and obtained deviations of 1.73 MHz and 0.286 dB in resonance frequencies and S11 parameters, respectively. The experimental results are shown in Fig. 19, which shows that the sensing property changes are negligible and insensitive to multiple experiments. Note that the S11 parameters of normal gasoline are less than −13 dB. To distinguish normal gasoline from HiDI gasoline regardless of temperature variation, a linear function is derived, as given in Equation (5).

$$\mathrm{f}\,(\mathrm{x}_1, \mathrm{x}_2) = \mathrm{x}_1 + 171.370\mathrm{x}_2 - 883.246 < 0 \tag{5}$$

where x_1 represents the S11 parameter less than −13 dB and x_2 represents the resonance frequency. Fig. 20 show the resonance frequency and S11 parameter against temperature as well as the plane corresponding to the function $\mathrm{f}\,(\mathrm{x}_1, \mathrm{x}_2)$ in Equation (5). Note that the resonance frequencies have a direct relation with temperature; resonance frequencies decline as the temperature decreases. Also, we can notice that the function can detect normal gasoline from HiDI gasoline with the minimum 4.40 MHz frequency margin and 0.764 dB S11 parameter margin to the closest sample. Since these margins are greater than the average standard deviation of measurements, we can expect the definite and stable distinction property of the proposed sensor.

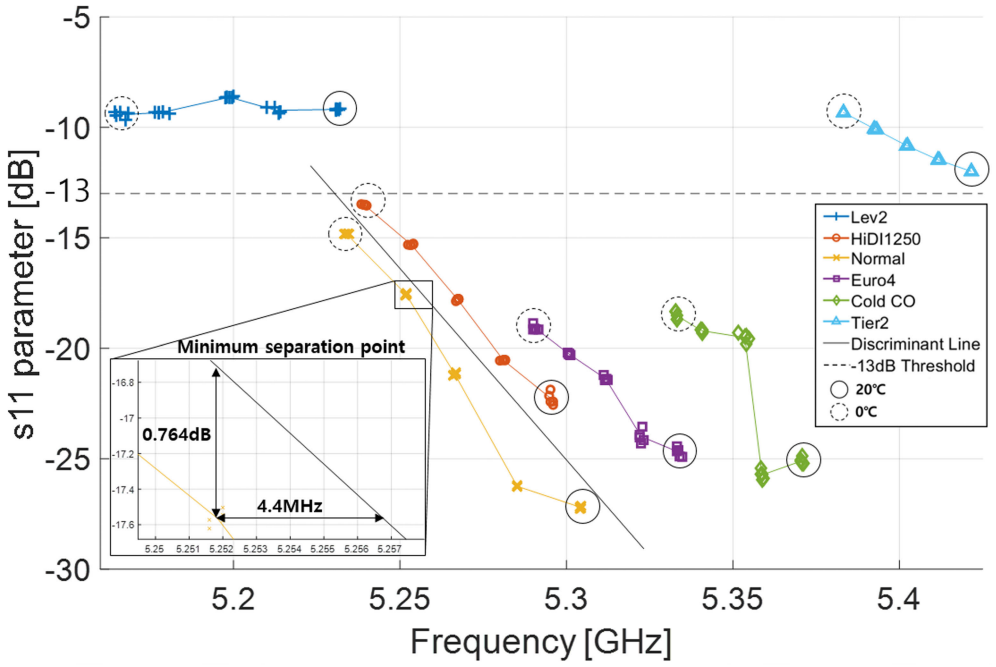

FIGURE 19. Resonant frequencies and s11 parameters of six gasoline samples at five temperatures obtained by five repetitive experiments.

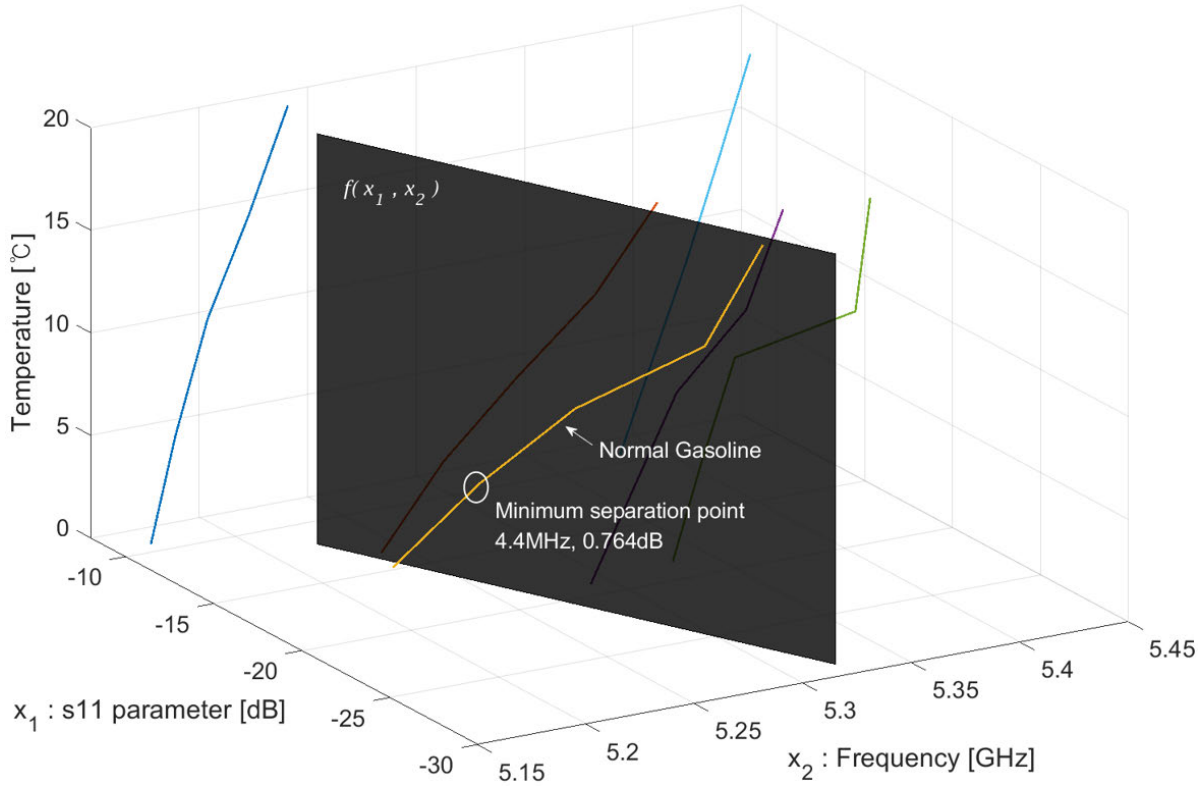

FIGURE 20. Resonant frequencies and s11 parameters at five temperatures with a decision plane.

IV. CONCLUSION

We propose a rectangular cavity sensor for the distinction of normal gasoline among HiDI gasolines. The proposed sensor is designed to have a high Q_{3dB} for large frequency separation between gasoline samples, and its design parameters are optimized and verified by HFSS simulations. The sensor is fabricated in simple rectangular form with a monopole at the center. The experiments at room temperature confirm

the proposed design and demonstrate effective normal gasoline detection capability. Experiments at various temperatures also show its robust distinction property to temperature variation by the distinction function of resonance frequency and S11 parameter. Through experiments according to design parameters and installation position locations, we show reliable, stable and repeatable properties of the proposed sensor. These results prove that the proposed sensor is significantly immune to temperature, position and design variations and thus can be effectively used for normal gasoline distinction.

REFERENCES

[1] S. Jorgensen, K. Eng, B. Evans, M. McNally, G. Musser, C. Richardson, D. Whelan, and E. Ziegel, "Evaluation of new volatility indices for modern fuels," SAE Tech. Paper 1999-01-1549, May 1999, doi: 10.4271/1999-01-1549.

[2] B. Evans, S. Jorgensen, G. Nusser, K. Eng, M. McNally, C. Richardson, D. Whelan, and E. Ziegel, "New gasoline volatility indices," *Automot. Eng.*, pp. 175–176, May 2000.

[3] H.-S. Lee, S. S. Wang, D. K. Lambert, J. Y. Lin, and C. R. Harrington, "An on-vehicle fuel driveability index sensor," *IEEE Sensors J.*, vol. 4, no. 6, pp. 722–727, Dec. 2004, doi: 10.1109/jsen.2004.837492.

[4] D. K. Lambert, C. R. Harrington, R. Kerr, H. S. Lee, Y. Lin, and S. C. Wang, "Fuel driveability index sensor," SAE Tech. Paper 2003-01-3238. Warrendale, PA, USA: SAE International, 2003.

[5] T. J. Ferguson, J. R. Griffin, and F. De Blauwe, "High DI fuel detection via exhaust gas temperature measurement for ULEV," SAE Tech. Paper 2000-01-0893. Warrendale, PA, USA: SAE International, 2000.

[6] G. W. Malaczynski, D. B. Miller, and S. L. Melby, "Low volatility fuel delivery control during cold engine starts," SAE Tech. Paper. 2005-01-0639, 2005, pp. 1–9, doi: 10.4271/2005-01-0639.

[7] A. Hassan, K. Lee, J. Bae, and C. H. Lee, "An inkjet-printed microstrip patch sensor for liquid identification," *Sens. Actuators A, Phys.*, vol. 268, pp. 141–147, Dec. 2017, doi: 10.1016/j.sna.2017.11.028.

[8] S. Kiani, P. Rezaei, M. Navaei, and M. S. Abrishamian, "Microwave sensor for detection of solid material permittivity in single/multilayer samples with high quality factor," *IEEE Sensors J.*, vol. 18, no. 24, pp. 9971–9977, Dec. 2018, doi: 10.1109/jsen.2018.2873544.

[9] Z. Meng, Z. Wu, and J. Gray, "Microwave sensor technologies for food evaluation and analysis: Methods, challenges and solutions," *Trans. Inst. Meas. Control*, vol. 40, no. 12, pp. 3433–3448, Aug. 2018, doi: 10.1177/0142331217721968.

[10] A. Babajanyan, J. Kim, S. Kim, K. Lee, and B. Friedman, "Sodium chloride sensing by using a near-field microwave microprobe," *Appl. Phys. Lett.*, vol. 89, no. 18, pp. 183504-1–183504-3, Oct. 2006, doi: 10.1063/1.2374681.

[11] G. Gennarelli, S. Romeo, M. R. Scarfi, and F. Soldovieri, "A microwave resonant sensor for concentration measurements of liquid solutions," *IEEE Sensors J.*, vol. 13, no. 5, pp. 1857–1864, May 2013, doi: 10.1109/jsen.2013.2244035.

[12] M. Hofmann, G. Fischer, R. Weigel, and D. Kissinger, "Microwave-based noninvasive concentration measurements for biomedical applications," *IEEE Trans. Microw. Theory Techn.*, vol. 61, no. 5, pp. 2195–2204, May 2013, doi: 10.1109/tmtt.2013.2250516.

[13] C. S. Oon, M. Ateeq, A. Shaw, A. Al-Shamma'a, S. N. Kazi, and A. Badarudin, "Experimental study on a feasibility of using electromagnetic wave cylindrical cavity sensor to monitor the percentage of water fraction in a two phase system," *Sens. Actuators A, Phys.*, vol. 245, pp. 140–149, Jul. 2016, doi: 10.1016/j.sna.2016.05.005.

[14] C. S. Oon, M. Ateeq, A. Shaw, S. Wylie, A. Al-Shamma'a, and S. N. Kazi, "Detection of the gas–liquid two-phase flow regimes using non-intrusive microwave cylindrical cavity sensor," *J. Electromagn. Waves Appl.*, vol. 30, no. 17, pp. 2241–2255, Nov. 2016, doi: 10.1080/09205071.2016.1244019.

[15] H. Guo, L. Yao, and F. Huang, "A cylindrical cavity sensor for liquid water content measurement," *Sens. Actuators A, Phys.*, vol. 238, pp. 133–139, Feb. 2016, doi: 10.1016/j.sna.2015.12.008.

[16] K. Saeed, R. D. Pollard, and I. C. Hunter, "Substrate integrated waveguide cavity resonators for complex permittivity characterization of materials," *IEEE Trans. Microw. Theory Techn.*, vol. 56, no. 10, pp. 2340–2347, Oct. 2008, doi: 10.1109/tmtt.2008.2003523.

[17] J. A. Cuenca, D. R. Slocombe, and A. Porch, "Temperature correction for cylindrical cavity perturbation measurements," *IEEE Trans. Microw. Theory Techn.*, vol. 65, no. 6, pp. 2153–2161, Jun. 2017, doi: 10.1109/tmtt.2017.2652462.

[18] M. Memon and S. Lim, "Microfluidic high-Q circular substrate-integrated waveguide (SIW) cavity for radio frequency (RF) chemical liquid sensing," *Sensors*, vol. 18, no. 2, p. 143, Jan. 2018, doi: 10.3390/s18010143.

[19] S. Karuppuswami, S. Mondal, M. I. M. Ghazali, and P. Chahal, "A multiuse fully 3-D printed cavity sensor for liquid profiling," *IEEE Sensors Lett.*, vol. 3, no. 2, pp. 1–4, Feb. 2019, doi: 10.1109/lsens.2018.2889761.

[20] C. H. Lee, Y.-S. Jeong, and H. Ashraf, "Cylindrical cavity sensor for distinction of various driveability index gasoline with temperature robustness," *Sensors*, vol. 19, no. 21, p. 4626, Oct. 2019, doi: 10.3390/s19214626.

[21] A. Webb, "Cavity- and waveguide-resonators in electron paramagnetic resonance, nuclear magnetic resonance, and magnetic resonance imaging," *Prog. Nucl. Magn. Reson. Spectrosc.*, vol. 83, pp. 1–20, Nov. 2014, doi: 10.1016/j.pnmrs.2014.09.003.

[22] B.-H. Liu, D. C. Chang, and M. T. Ma, "Eigenmodes and the composite quality factor of a reverberating chamber," Inist-CNRS., Vandœuvre-lès-Nancy, France, Tech. Rep., no. 9541100, 1983, no. 1066.

[23] M. T. Sebastian, M. A. S. Silva, and A. S. B. Sombra, "Measurement of microwave dielectric properties and factors affecting them," in *Microwave Materials and Applications 2V Set*, M. T. Sebastian, H. Jantunen, and R. Ubic, Eds. Chichester, U.K.: Wiley, 2017, p. 1e51.

[24] A. A. Carey and A. J. Hayzen. (2013). *Machinery Lubrication-The Relative Permittivity and Oil Analysis*. Emerson Process Management. Accessed: Aug. 20, 2020. [Online]. Available: http://www.Machinerylubrication.com/Read/226/dielectric-constant-oil-analysis

CHONG HYUN LEE (Member, IEEE) received the B.S. degree in electronic engineering from Hanyang University, in 1985, the M.S. degree from Michigan Technological University, in 1987, and the Ph.D. degree in electronic engineering from the Korea Institute of Science and Technology (KAIST), in 2002. He is currently working as a Professor with the Department of Ocean System Engineering, Jeju National University. His research interests include smart RF sensor design, acoustic and sonar signal processing, and machine learning.

YOONSANG JEONG received the B.S. degree from Jeju National University, in 2012, where he is currently pursuing the master's degree with the Department of Ocean System Engineering. His research interests include smart RF sensor design, signal processing, and energy harvesting.

HINA ASHRAF received the B.S. degree in telecommunication engineering and the M.S. degree in electrical engineering from the National University of Computer and Emerging Sciences (NUCES-FAST), in 2010 and 2014, respectively. She is currently pursuing the Ph.D. degree with the Department of Ocean System Engineering, Jeju National University. Her research interests include sonar signal processing and audio signal generation using machine learning.